

Theoretical Analysis of Damping Due to Air Viscosity in Narrow Acoustic Tubes

M. Watanabe, T. Yamaguchi, M. Sasajima, Y. Kurosawa and Y. Koike

Abstract—Headphones and earphones have many extremely small holes or narrow slits; they use sound-absorbing or porous material (i.e., dampers) to suppress vibratory system resonance. The air viscosity in these acoustic paths greatly affects the acoustic properties. Simulation analyses such as the finite element method (FEM) therefore require knowledge of the material properties of sound-absorbing or porous materials, such as the characteristic impedance and propagation constant. The transfer function method using acoustic tubes is a widely known measuring method, but there is no literature on taking measurements up to the audible range. To measure the acoustic properties at high-range frequencies, the acoustic tubes that form the measuring device need to be narrowed, and the distance between the two microphones needs to be reduced. However, when the tubes are narrowed, the characteristic impedance drops below the air impedance. In this study, we considered the effect of air viscosity in an acoustical tube, introduced a theoretical formula for this effect in the form of complex density and complex sonic velocity, and verified the theoretical formula. We also conducted an experiment and observed the effect from air viscosity in the actual measurements.

Keywords—acoustic tube, air viscosity, earphones, FEM, porous material, sound-absorbing material, transfer function method

I. INTRODUCTION

HEADPHONES and earphones have many extremely small holes or narrow slits. We use sound-absorbing or porous material (i.e., dampers) to suppress vibratory system resonance. The air viscosity in these acoustic paths greatly affects acoustic properties. With the current advances in computer speed and capacity, CAE(Computer Aided Engineering) technology is also becoming widely used in the acoustics field, but there are few examples of analysis of sound propagation characteristics in small spaces such as those in earphones or headphones up to the audible range (20 Hz–20 kHz).

Simulations must consider the effect of the material properties of sound-absorbing or porous materials. To include the effects of sound-absorbing and porous materials into simulations, such as the finite element method (FEM), the characteristic impedance Z_c and propagation constant γ , which

are the physical properties of the attenuation material, are required. The transfer function method can be used for the characteristic impedance and propagation constants of sound-absorbing or porous materials, in the range of 200 Hz–6 kHz, but, measurements in the audible range (i.e. 20–20kHz) are not possible with commercial acoustic tubes. Moreover, there is presently no literature available on the material properties of attenuation materials up to 20 kHz.

To measure the material properties over a high range, the acoustic tubes need to be narrowed, and the distance between two microphones needs to be shortened. However, the effect of narrowing the tubes on air viscosity between the tube wall and air when a wave is propagated in the tube cannot be disregarded. In this study, we first derived a theoretical formula regarding the effect of air viscosity inside acoustic tubes and then reported on the results of an experiment to verify its effectiveness.

II. THEORETICAL ANALYSIS FOR ACOUSTIC TUBES

The sound pressure inside an acoustic tube can be derived from the wave motion equation. It can be derived from the equation for closed acoustic tubes as follows:

$$P = j\rho_0 c_0 u_0 e^{j\omega t} \frac{\cos k(l - x_m)}{\sin kl} \quad (1)$$

where P is the sound pressure, ρ_0 is the air density, c_0 is the sound speed in air, ω is the angular frequency, u_0 is the velocity amplitude of the vibrating surface, k is the wave number, l is the total length of the acoustic tube, and x_m is the distance between the end of the tube and microphone. This is an ideal equation that does not consider the air viscosity.

We considered the particle velocity distribution in the radial direction (y direction) of the tube. According to Biot [1], [2], the two dimensional particle velocity distribution of a sound wave in the radial direction (y direction) in the acoustic tube is expressed by (2):

$$U_1 = \frac{X}{j\omega} \left\{ 1 - \frac{\cosh \left[\left(\frac{j\omega}{\nu} \right)^{\frac{1}{2}} y \right]}{\cosh \left[\left(\frac{j\omega}{\nu} \right)^{\frac{1}{2}} a_1 \right]} \right\} \quad (2)$$

M. Watanabe, Y. Koike, and M. Sasajima are with the Strategic Research & Development Division, Foster Electric Co., Ltd., 196-8550, 1-1-109 Tsutsujigaoka, Akishima, Tokyo, Japan (phone: 042-847-3334; e-mail: {mtwatanabe, koike, sasajima}@foster.co.jp).

T. Yamaguchi is with the Department of Mechanical System Engineering, Gunma University, 376-8515, 1-5-1, Tenjin-cho, Kiryu, Gunma, Japan (e-mail: yamagme3@gunma-u.ac.jp).

Y. Kurosawa is with the Department of Precision Mechanical System Engineering, Teikyo University, 320-8551, 1-1, Toyosatodai, Utsunomiya, Tochigi, JAPAN (e-mail: ykurosawa@mps.teikyo-u.ac.jp).

where U_1 is the relative velocity between the tube's longitudinal component of the particle velocity of the air inside the tube and longitudinal movement velocity of the tube wall. Since the tube wall velocity in this example is zero, U_1 is equal to the longitudinal component of the particle velocity of the air inside the tube. a_1 is the tube's radius, ν is the kinematic viscosity of the air, j is an imaginary unit, and X is a y -independent function. When this velocity distribution is visualized as a graph, as shown in Fig. 1, the horizontal axis represents position y in the tube's radial direction, and the origin is the tube's center. The vertical axis represents the particular velocity distribution for the particle velocity graphs at 100 Hz and 1 kHz. Quadratic curve-like behavior can be seen, especially when the tube is extremely narrow and in the low 100 Hz range. As it moves into the high frequencies, it becomes a plane wave shape, but a steep distribution is found near the tube wall.

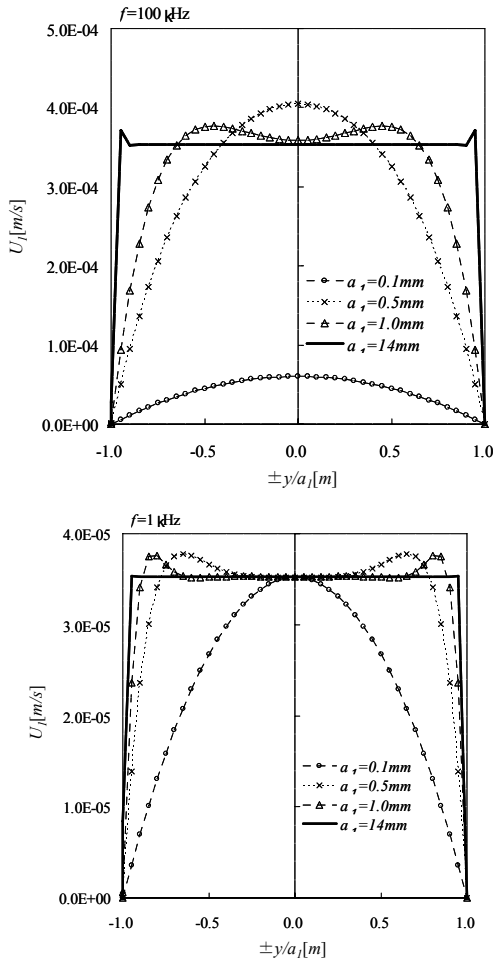


Fig. 1 Particle velocity distribution

When calculating the sound speed and air density from this particle velocity distribution, the following equations are used for the complex sound speed and complex density[3]-[5]:

$$\rho^* = \rho_0 + \left(\frac{12\mu}{j\omega d^2} \right) \frac{\frac{1}{3}\beta \tanh(\beta)}{1 - \left(\frac{1}{\beta} \right) \tanh(\beta)} \quad (3)$$

$$c^* = \sqrt{\frac{\gamma P_a}{\rho^*}} \quad (4)$$

where β is expressed as follows:

$$\beta = \frac{d}{2} \sqrt{\frac{j\omega \rho_0}{\mu}} \quad (5)$$

μ is the air viscosity coefficient, γ is the specific heat ratio, P_a is the atmospheric pressure, and d is the tube diameter. When we substitute the sound speed c_0 , air density ρ_0 , and wave number k of Eq. (1) into the theoretical equation for sound pressure inside acoustic tubes with complex sonic velocity c^* , complex density ρ^* , and complex wave number k^* , we obtain (6) and thus derive a theoretical expression that considers the effect of air viscosity:

$$P^* = j\rho^* c^* u_0 e^{j\omega t} \frac{\cos k^*(l - x_m)}{\sin k^* l} \quad (6)$$

Fig. 2 compares the graphs of SPL (Sound pressure Level) for the theoretical equation using conventional air density and sound speed and the theoretical equation proposed in this paper. The white circles in the graphs are the conventional calculation results without viscosity, and the solid lines are the results with viscosity. Because of the experiment, which is outlined in the next section, we used a tube length of $l = 248.8$ mm; observation points were assumed to be the microphone positions $x_m = 221.8$ and 234.8 mm, and the tube diameter $d = 14$ mm. The graphs clearly show that resonance was extremely sharp because resistance due to air viscosity was not considered in the theoretical equation derived from the general wave equation. In contrast, when the theoretical equation utilized the complex sound speed and complex density of a $d = 14$ mm tube, the sound pressure at the graph's resonance points diminished, and resonance sharpness was suppressed.

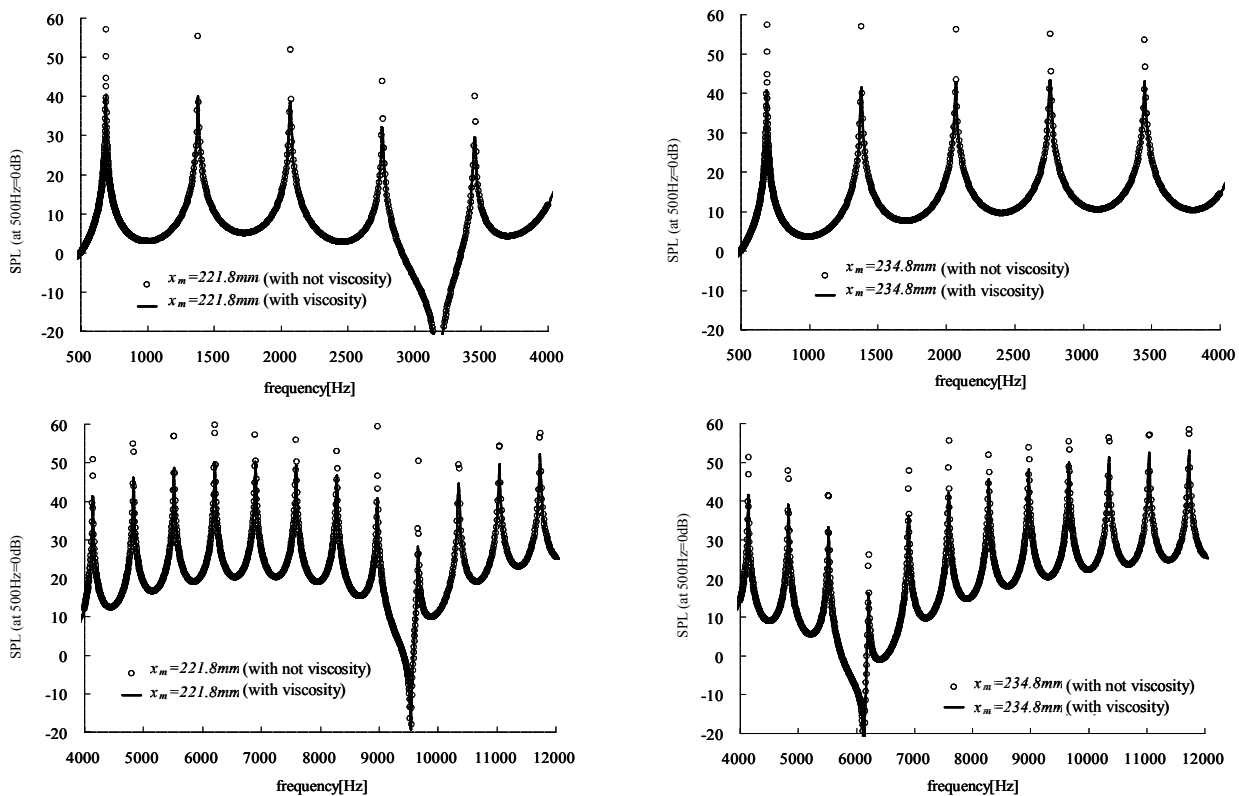


Fig. 2 Theoretical curves of sound pressure level

When we focused on certain resonance points, we observed changes in attenuation when we changed the tube diameter. Fig.3 shows the property changes for the resonance points when the tube diameter was changed. As the diameter was decreased, the sound pressure at the resonance peak was suppressed, the resonance frequency decreased, and the resonance positions changed in line with the left part of the conventional theoretical curve.

Thus, we were able to express the attenuation of sound waves inside an acoustic tube by deriving a theoretical equation that makes use of complex density and complex sound speed.

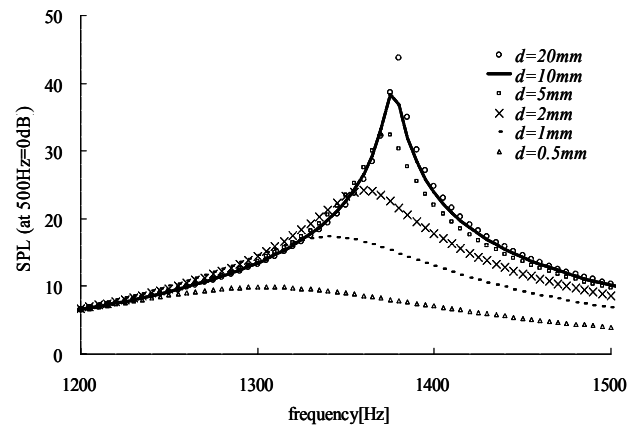


Fig. 3 Changes in resonance points due to diameter of tube

III. EXPERIMENT METHOD

Fig. 4 shows the measurement system using acoustic tube. Most commercially available acoustic tubes have diameters of $\phi 29$ – 100 mm. We used a $\phi 14$ mm acoustic tube with a distance between microphones of 13 mm; we measured the characteristic impedance up to 12 kHz and considered the propagation constant by transfer function method. Since we wanted to measure the effect of the tube wall due to air viscosity, we simply closed the tube ends with a rigid wall to form a closed

tube and measured the sound pressure with two microphones. Theoretical computation of the speaker behavior is difficult when speakers are used as a sound source, whereas use of a 1/2-in condenser microphone ensures a sound source of constant displacement with no need to consider the effect of the sound source. The tube length was 248.8 mm, and the distance between the 1/2 in microphone forming the speaker and 1/4 in microphone on the other side was 221.8 mm. The M series white noise was used as the sound source, and output signals were analyzed with a Fast Fourier transform (FFT) analyzer. Fig. ure 5 shows a photograph of the actual experimental setup.

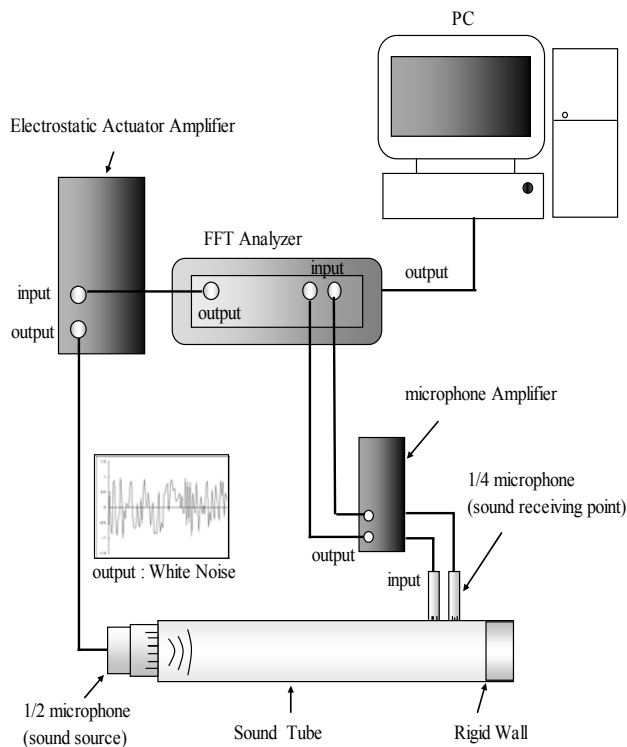


Fig. 4 Measurement system

IV. EXPERIMENT RESULTS

The experiment results are shown in Fig. 6. For clarity, frequencies are shown separately, similar to the theoretical value graphs. The top graphs show the frequency

characteristics of the sound pressure at a distance of $x_m = 221.8$ mm from the sound source, and the bottom graphs show them at a distance of $x_m = 234.8$ mm from the sound source. The resonance points from the length of the tube appeared approximately every 700 Hz. No steep peaks were seen for resonance points, and attenuation from viscosity was observed. These experiment results were consistent with the trends in the theoretical analysis results.



Fig. 5 Experimental setup

V. CONCLUSION

We examined the effect of air viscosity on narrow acoustic tubes with regards to acoustic tube measurements based on actual measurements and a theoretical analysis.

We derived the complex sound speed and complex density from the particle velocity distribution inside the tube and applied them to a theoretical equation for closed acoustic tubes. Sharp resonance was suppressed when the tube diameter was reduced. Moreover, the resonance points in the conventional theoretical equation showed that the resonance frequency decreased in line with the low frequency side of the resonance peak.

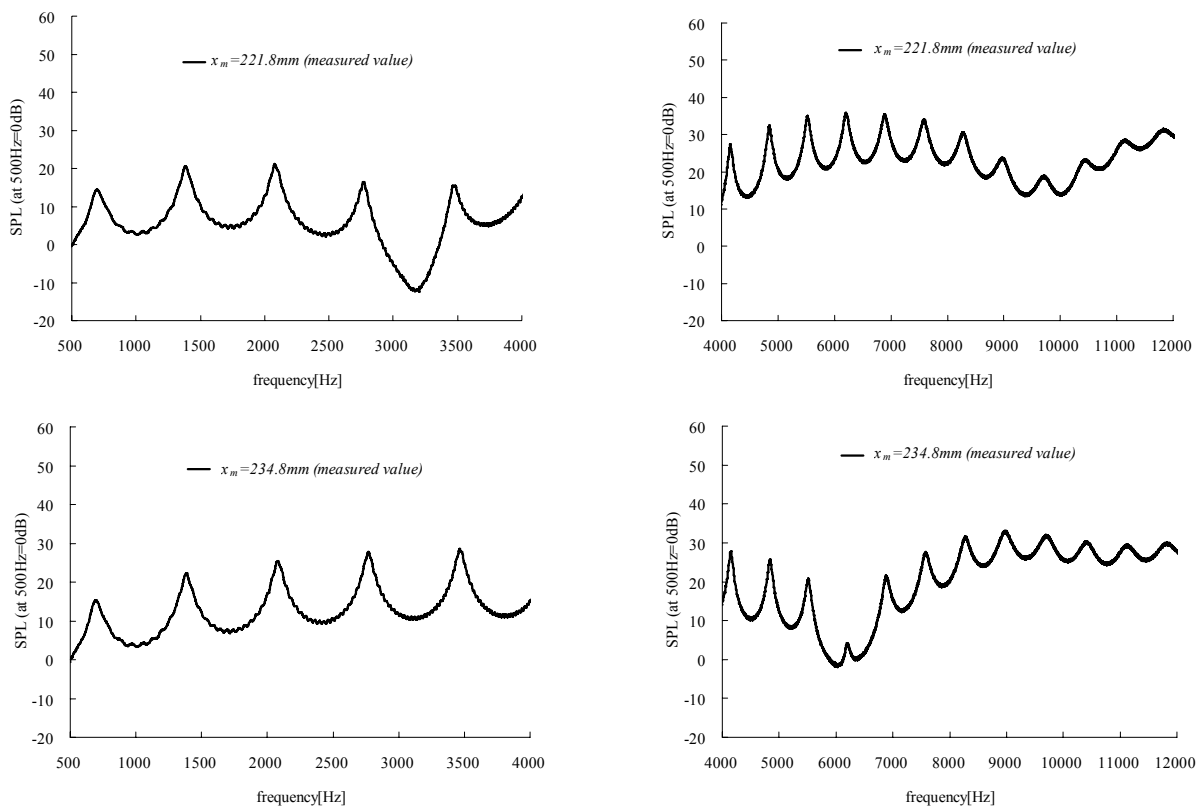


Fig. 6 Experimental curves of sound pressure level

By using a microphone as the sound source in the actual measurements, we were able to realize a sound source of constant displacement; this enabled evaluation that was independent of the sound source properties. The actual measured results for the resonance frequency and trends were consistent with the theoretical values. Since sharp resonance was suppressed with a tube diameter of 14 mm due to the use of a 1/2 in microphone as a sound source, we were able to observe in the experiment that the resistance due to air viscosity had a great effect in the case of narrow tubes, as predicted theoretically. In the future, we will verify this further using narrow tube and extend our work to transfer function method calculations for material property measurements.

REFERENCES

- [1] M. A. Biot, *Acoustics, Elasticity, and Thermodynamics of Porous Media*. Woodbury, New York: Acoustical Society of America, 1992.
- [2] M. A. Biot, "Theory of propagation of elastic waves in a fluid-saturated porous solid II: Higher frequency range," *Journal of the Acoustical Society of America*, vol. 28, pp. 179–191, 1956.
- [3] H. Utsuno, Ting W. Wu, and A. F. Seybert "Prediction of Sound Fields in Cavities with Sound Absorbing Materials", *AIAA Journal*, vol.28-11, pp1870-1875, 1990.
- [4] H. Utsuno, T. Tanaka, T. Fujikawa "Transfer function method for measuring characteristic impedance and propagation constant of porous materials", *Journal of the Acoustical Society of America*, vol. 86-2, pp. 637–643, 1989.
- [5] J. F. Allard and N. Atalla, *Propagation of Sound in Porous Media*. West Sussex, UK: John Wiley & Sons, Ltd., 2009.